The Role of Ni in Sulfided Carbon-Supported Ni–Mo Hydrodesulfurization Catalysts

S. M. A. M. Bouwens,[1] N. Barthe-Zahir, V. H. J. de Beer, and R. Prins[2]

Laboratory for Inorganic Chemistry and Catalysis, Eindhoven University of Technology, P.O. Box 513, 5600 MB Eindhoven, The Netherlands

The thiophene hydrodesulfurization activities of Ni and Ni–Mo sulfide catalysts supported on activated carbon were measured at atmospheric pressure and the catalyst structures were studied by means of X-ray photoelectron spectroscopy, dynamic oxygen chemisorption, and chemical sulfur analysis. The Ni/C catalysts contained a Ni_3S_2-like phase which, due to the impregnation method, was considerably enriched in the outer shell of the carbon support grains. Both for the Ni/C and Ni–Mo/C catalysts no correlation was observed between the dynamic oxygen chemisorption and the catalytic activity and for the Ni/C catalysts indications for full oxidation of the Ni_3S_2 particles were obtained. The specific catalytic activity per Ni atom was lower in the Ni/C catalysts than in the Ni–Mo/C catalysts. Since the local Ni structure in these catalysts is different, however, it proved not possible to decide whether the Ni atoms in Ni–Mo/C catalysts are the actual active sites or not. © 1991 Academic Press, Inc.

INTRODUCTION

Catalysts based on molybdenum or tungsten sulfide and promoted by nickel or cobalt have been used extensively for hydrotreating in petroleum refining for many years. Intensive research aiming at clarification of the nature of the active phases and especially at the role of the Co and Ni promoters has resulted in many different views with regard to the catalytic synergy in Co(Ni)–Mo(W) catalysts (*1*). At present the "Co–Mo–S" model is strongly favored since a relationship could be established between the hydrodesulfurization (HDS) activity and the amount of promoted active phase for a wide range of Co–Mo catalysts, either unsupported (*2*) or dispersed on different supports (*3, 4*). It has been observed that Co–Mo–S-type structures are not restricted to Co–Mo systems, but that they are also present in alumina-supported Co–W (*5*), Fe–Mo (*5–8*), and Ni–Mo (*9–12*) catalysts.

Although the structure of the Co–Mo–S sites has been elucidated by recent EXAFS studies of Co–MoS_2 (*13*) and Ni–MoS_2 (*14, 15*) catalysts, the exact catalytic nature of the active sites is still under discussion. For instance, it is unclear whether the neighboring Mo atoms in the active Co–Mo–S and Ni–Mo–S sites play a direct role in the HDS reactions, or whether the catalysis is solely determined by the Co, or Ni, promoter atoms. The relevance of this last possibility was clearly pointed out by Duchet *et al.* (*16*) and Vissers *et al.* (*17*) who studied thiophene HDS of carbon-supported Co, Mo, and Co–Mo catalysts. On the basis of the remarkably high HDS activity of Co/C, Vissers *et al.* demonstrated that the promoter effect in sulfided Co–Mo catalysts can completely be explained by the high catalytic activity of the cobalt sites. Consequently, in their model the role of MoS_2 is mainly to function as a support for optimally dispersed cobalt atoms. The authors arrived

at their conclusions from the estimated intrinsic activity of optimally dispersed cobalt sulfide in Co/C catalysts, which turned out to be nearly equal to the catalytic activity of a promoted Co–Mo/C catalyst. The latter model assumes that the structure of the active cobalt sites in a Co/C catalyst is similar to that in a Co–Mo/C catalyst. Very recently this assumption was supported by a Mössbauer emission spectroscopy study of a sulfided Co/C and a Co–Mo/C catalyst (*18, 19*), in which similar Mössbauer spectra were obtained for both catalysts.

In view of the analogy between Co–Mo–S and Ni–Mo–S type structures, it seemed of interest to investigate whether the catalytic activity of Ni-promoted Mo sulfide catalysts can also be attributed to the activity of the promoter atoms. Therefore, in the present study the structure and HDS activity of carbon-supported Ni catalysts has been compared with the corresponding promoted Ni–Mo catalysts. For this purpose the intrinsic activity of the active nickel sites in sulfided Ni/C catalysts as well as in sulfided Ni–Mo/C catalysts were estimated. Structural information of the active phases was provided by X-ray photoelectron spectroscopy (XPS), dynamic oxygen chemisorption (DOC), and chemical sulfur analysis.

EXPERIMENTAL

Catalytic Activity

Series of Ni/C catalysts (0.6–14.8 wt% Ni), Mo/C catalysts (1.4–7.0 wt% Mo), and promoted Ni–Mo/C catalysts (0.5–6.1 wt% Ni, 4.1–4.8 wt% Mo) were prepared analogously to the Co catalysts described before (*13*). Catalyst samples are denoted as Ni(x)–Mo(y)/C, with x and y representing the wt% Ni and Mo, respectively. Catalytic activity for thiophene HDS was tested in a flow microreactor operating at 673 K and atmospheric pressure. Catalyst samples (0.2 g) were sulfided *in situ* for 2 h at 673 K in a mixture of H_2S/H_2 (1:9) (*13*). After sulfidation, the reaction mixture consisting of 6.2 mol% thiophene in hydrogen was in-

troduced at a flow rate of 50 cm^3 min^{-1}. The concentrations of the reaction products measured after 2 h were used to calculate the first-order rate constants for the HDS and the consecutive butene hydrogenation (HYD) reactions.

X-Ray Photoelectron Spectroscopy (XPS)

XPS spectra of the dried oxidic Ni/C samples were recorded on a Physical Electronics 550 XPS/AES spectrometer equipped with a Mg anode ($E = 1253.6$ eV) and a double-pass cylindrical mirror analyzer operating at a pass energy of 100 eV. XPS spectra of the sulfided Ni/C samples were recorded on an AEI ES 200 spectrometer equipped with a Al anode ($E = 1486.6$ eV) and a spherical analyzer operating at a pass energy of 60 eV. After sulfidation, carried out as described above, the catalyst samples were flushed with purified He for 15 min at 673 K and subsequently cooled to room temperature. The C 1s peak (284.6 eV) was used as an internal standard for binding energy calibration and the Ni-over-C photoelectron intensity ratios were used to measure the degree of dispersion of the Ni phase on the support. The intensities of the C 1s peak and the Ni 2p multiplet peaks (including shake-up structures) were calculated using a linear baseline. Theoretical intensity ratios were calculated as described before (*13*).

Dynamic Oxygen Chemisorption (DOC)

Dynamic oxygen chemisorption measurements at atmospheric pressure were carried out in a similar microreactor as used for the thiophene HDS activity test. Catalyst samples (0.2 g) were sulfided *in situ* in the same manner as described above. The freshly sulfided samples were purged in purified He for 15 min at 673 K and subsequently cooled to 333 K within 90 min in a He flow (30 ml min^{-1}). Oxygen chemisorption was then measured at 333 K (*11, 12, 20*) by injecting 2.13-ml pulses of a 5.0 mol% O_2 in He mixture at 4.5 min intervals into the

BOUWENS ET AL.

He carrier gas flow. When effluent O_2 peaks had increased to constant size (less than 1% difference between two successive peaks) the total O_2 uptake was calculated.

Chemical Sulfur Analysis

The total sulfur content of the freshly sulfided catalysts was determined by combustion of the *in situ* sulfided catalysts (sulfided and flushed according to the procedure described for the DOC measurements) in a 25 mol% O_2 in He gas flow (150 ml min^{-1}). The following temperature program was applied: starting at about 373 K the temperature was increased linearly at a rate of 10 K min^{-1} until 1073 K, where it was kept constant for 60 min. The emerging SO_2 and SO_3 were trapped in two vessels containing an ice-cooled aqueous solution of H_2O_2 (1%). The total sulfur content was measured by titrating the sulfuric acid with a solution of 0.01 M PbClO$_4$, using a lead-selective electrode.
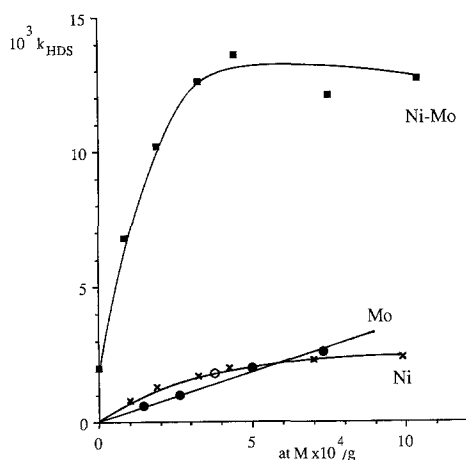

FIG. 1. Reaction rate constants k_{HDS} for the HDS of thiophene as a function of Ni loading for the Ni/C and Ni–Mo/C catalysts, and as a function of Mo loading for the Mo/C catalysts. The activity of a Ni/C catalyst, prepared by impregnation with Ni(NH$_3$)$_6^{2+}$ in ammonia, is indicated by an open circle.

RESULTS

Catalytic Properties

The catalytic activities of the Ni/C, Mo/C, and Ni–Mo/C catalysts are presented in Table 1 and Fig. 1. The thiophene HDS activities of the promoted Ni–Mo/C catalysts are much higher than those of the various Ni/C and the Mo(4.8)/C catalysts and there is a maximum at a Ni/Mo atomic ratio of about 1. With regard to the hydrogenation capacity the k_{HYD}/k_{HDS} ratio was found to decrease rapidly with a small amount of nickel (Ni/Mo < 0.2) and more slowly for larger Ni/Mo ratios. Furthermore, the k_{HYD}/k_{HDS} ratios of the Ni–Mo/C catalysts were found to be significantly lower than that of Mo(4.8)/C and slightly lower than those of the Ni/C catalysts. Dynamic oxygen chemisorption measurements were carried out for the entire loading range of the sulfided Ni/C, Mo/C, and Ni–Mo/C catalysts. The results are presented in Table 1 and Fig. 2. The DOC values of the Ni/C and Mo/C catalysts remained negligible up to 0.6 wt% Ni and 1.4 wt% Mo, respectively,
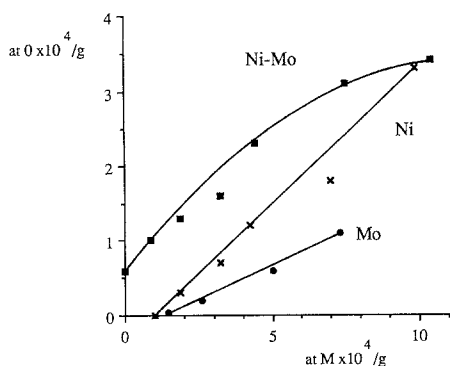
TABLE 1

Thiophene HDS Rate Constants (k_{HDS}), Ratios of the Hydrogenation and HDS Rate Constants (k_{HYD}/k_{HDS}), and Dynamic Oxygen Chemisorption Characteristics of Sulfided Carbon-supported Ni, Mo and Ni–Mo Catalysts

Catalyst composition (wt%)		Catalytic activities		Chemisorption DOC × 10^4 (at. O g^{-1})
Ni	Mo	k_{HDS} × 10^3 (m^3 kg^{-1} s^{-1})	k_{HYD}/k_{HDS}	
0.6	—	0.8	1.4	0
1.1	—	1.3	1.8	0.3
1.9	—	1.7	1.4	0.7
2.5	—	2.0	1.3	1.2
4.1	—	2.3	1.2	1.8
5.8	—	2.4	1.3	3.3
10.6	—	2.8	1.0	7.5
14.8	—	2.7	0.9	7.4
—	1.4	0.6	4.8	0.04
—	2.5	1.0	3.4	0.2
—	4.8	2.0	2.4	0.6
—	7.0	2.6	2.4	1.1
—	4.8	2.0	2.4	0.6
0.5	4.8	6.8	0.9	1.0
1.1	4.3	10.2	0.7	1.3
1.9	4.4	12.6	0.7	1.6
2.6	4.4	13.6	0.6	2.3
4.4	4.9	12.1	0.6	3.1
6.1	4.1	12.7	0.5	3.4

FIG. 2. Oxygen chemisorption values as a function of Ni loading for the Ni/C and Ni–Mo/C catalysts, and as a function of Mo loading for the Mo/C catalysts.

and thereafter increased linearly with metal loading up to the maximum loading. The DOC values of the Ni–Mo/C catalysts increased linearly with Ni loading up to 2.6% Ni and then increased less strongly.

Sulfur Analysis

The sulfur-to-metal stoichiometries were determined by chemical sulfur analysis. The S/Ni ratios amounted to 0.62, 0.73, and 0.79 for the Ni(4.1)/C, Ni(5.8)/C, and Ni(10.6)/C catalysts, respectively. These ratios are subject to some uncertainty, since they were determined by subtracting the amount of sulfur contained on the pure carbon support (determined to be 0.8 wt% S in a separate experiment) from the total amount of sulfur determined in the Ni/C catalysts.

About 0.4% of this sulfur was already present in the untreated carbon support and an additional 0.4% is taken up during the sulfidation treatment. The uncertainty comes from the fact that it is unknown if the presence of the metal sulfides influences this additional sulfur uptake. For the Ni(4.1)/C catalyst the contribution of the additional 0.4% sulfur on the support to the total sulfur content is as high as 19%. For the high loading Ni(10.6)/C catalyst, however, the S/Ni ratio could be determined much more accurately since this support sulfur contribution was only 8%. The S/Ni ratios between 0.62

and 0.79 point to a Ni_3S_2 rather than a NiS stoichiometry. A S/Mo ratio of 1.92 was obtained for the sulfided Mo(4.8)/C catalyst. The S/(Ni + Mo) ratios for the sulfided Ni–Mo/C catalysts are presented in Fig. 3 as a function of the Ni/Mo ratio and compared with the predicted ratios, assuming that the metal-to-sulfur stoichiometries of Ni and Mo in these catalysts are as in Ni_3S_2 and $MoS_{1.92}$, respectively. It is clear that the Ni(x)–Mo(4.8)/C catalysts are richer in sulfur than a physical mixture of Ni(x)/C and Mo(4.8)/C sulfided under the same conditions.

XPS

XPS spectra were recorded for the entire Ni loading range of the Ni/C catalysts, in the dried precursor state as well as in the sulfidic state. The Ni $2p_{3/2}$ peak in the precursor catalysts is situated at 855.6 ± 0.2 eV. This binding energy is high compared to that of NiO (853.3 eV, *(21)*) and is close to that of $Ni(NO_3)_2$ (856.9 eV, *(21)*), indicating that at least part of the Ni ions are still associated with nitrate ions. A similar observation was made for Co/C *(17)* and Fe/C catalysts *(22–24)*. In the sulfided state the binding energy of the Ni $2p_{3/2}$ peak was in the range 853.2–853.7 eV, and of the S $2p$ peak in the range 162.6–162.9 eV. These Ni $2p_{3/2}$ values compare with the literature
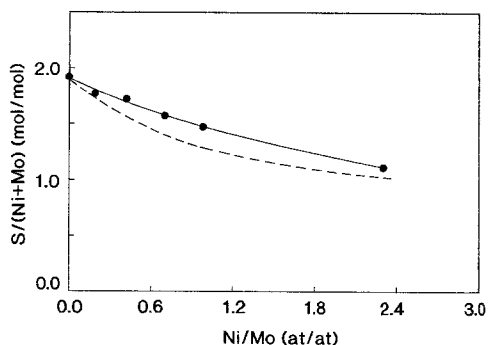

FIG. 3. S/(Ni + Mo) molar ratio of Ni–Mo/C catalysts as a function of the Ni/Mo ratio. The dashed curve represents the S content calculated for a physical mixture of Ni_3S_2 and $MoS_{1.92}$ with varying Ni/Mo ratio.
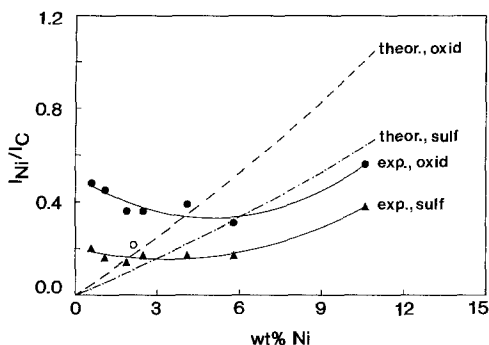
FIG. 4. Experimental Ni $2p$/C $1s$ XPS intensity ratios of the oxidic (●) and sulfided (△) Ni/C samples as a function of Ni loading, and the theoretical intensity ratios predicted for 100% dispersion (27). A catalyst prepared by impregnation of carbon with $Ni(NH_3)_6^{2+}$ in ammonia, and measured in the oxidic state, is denoted by an open circle.

value of 853.7 eV for Ni_3S_2 reported by Ng and Hercules (25) and Broutin et al. (26) better than with the values of 854.2 (25) and 854.0 (26) reported for NiS. The values of 162.6–162.9 eV for the S $2p$ peak binding energy are in the range expected for metal sulfides (21). From the experimental Ni and S $2p$ intensity ratios, atomic sulfur-to-nickel ratios can be calculated after subtraction of the amount of elemental sulfur formed during sulfidation of the carbon support itself (I_S/I_C = 0.003, (17)). S/Ni ratios ranging from 0.6 to 0.8 were obtained for the Ni/C catalysts, which also point to the presence of Ni_3S_2.

Information about the dispersion of the Ni phase can be obtained by comparing the ratios of the experimental Ni $2p$ to C $1s$ intensities with the theoretical ratios predicted by the quantitative XPS model of Kuipers (27). This model is applicable for the determination of the dispersion of catalytic phases of any shape, which are homogeneously deposited on the carrier surface. In Fig. 4 the experimental intensity ratio and the theoretical intensity ratio, calculated under the assumption of 100% dispersion, are presented. The following features can be discerned:

—At low Ni loadings (up to approximately 4 wt% Ni in the oxidic state and 3 wt% Ni in the sulfided state), the experimental intensity ratios for the Ni/C catalysts are in excess of the theoretical values.

—The experimental intensity ratios of the sulfided Ni/C catalysts are lower than those of the corresponding oxidic samples.

—Up to approximately 6 wt% Ni a slight decrease in the experimental intensity ratio for the oxidic Ni/C samples is observed with increasing Ni loading, while the theoretical intensity ratios increase. The sulfided samples exhibit a nearly constant intensity ratio in this Ni-loading range.

Since the theoretical Ni-to-C intensity ratios have been calculated under the assumption of complete dispersion, these ratios are the maximum values that can be reached for homogeneous samples at a given Ni content. The observation that the experimentally determined intensity ratios of the oxidic and the sulfided samples are higher than the theoretical ones, therefore, leads to the conclusion that the Ni phase present in the Ni/C catalysts is not uniformly deposited on the support surface and, more specifically, that a considerable enrichment of Ni at the outside of the support grains has occurred, especially at low Ni loading.

In a previous XPS investigation (28) we have observed that the molybdenum distribution in oxidic and sulfided Mo/C catalysts is homogeneous and that the final MoS_2 particles are reasonably small. Since the Ni atoms in the Ni–Mo–S phase are situated at the edges of the MoS_2 particles, the Ni distribution in sulfided Ni–Mo/C catalysts should also be homogeneous. XPS intensity measurements on Ni–Mo/C catalysts were not in contradiction with this conclusion.

DISCUSSION

Since catalyst dispersion should be maximal at low metal contents, the specific activity of an optimally dispersed metal sulfide might be obtained by determining the slope of the k_{HDS} versus metal loading curve at 0

wt% metal (17). For this purpose, the data points of the thiophene HDS reaction rate constants as a function of the weight percentages of Ni (Ni/C, and Ni–Mo/C with 4.8 wt% Mo) and of Mo (Mo/C) were curve-fitted with a second-order polynomial, and the derivative was determined at 0 wt% metal. The specific activities per Ni atom amounted to 9 mmol $mol^{-1} s^{-1}$ for Ni/C and 60 mmol $mol^{-1} s^{-1}$ for Ni–Mo/C, while the specific activity per Mo active site in Mo/C was 4 mmol $mol^{-1} s^{-1}$. The relative accuracy of these values is about 10%. Whereas the specific activity of a Co site in Co/C compared well with that in Co–Mo/C (17), the specific activity of a Ni site in Ni/C is much lower than in Ni–Mo/C. In contrast to Co, it thus seems as if the increased activity of the promoted Ni–Mo/C catalysts cannot be ascribed to the Ni atoms only. Three explanations can be given for this fact:

(i) The Ni atoms in the Ni–Mo/C catalysts are not the active sites;
(ii) the calculated specific activity of Ni in the Ni/C catalysts is too low;
(iii) a difference exists between the local structure of the Ni atoms in Ni/C and Ni–Mo/C, resulting in a different specific thiophene HDS activity.

Mo EXAFS results demonstrated that all Mo atoms in a Ni–Mo/C catalyst which had all Ni atoms in the Ni–Mo–S structure, are fully surrounded by S atoms (14). This suggests that the Mo atoms are not accessible to gaseous molecules and that the Ni rather than the Mo atoms are acting as the catalytic sites in the promoted catalysts. In accordance with this, the observed k_{HYD}/k_{HDS} ratios of the Ni–Mo/C catalysts are more in line with those of the Ni/C catalysts than with that of the Mo(4.8)/C catalyst (Table 1). Similarly, in the case of Co–Mo/C catalysts it was found that the k_{HYD}/k_{HDS} ratios were very close to those of the Co/C catalysts while differing substantially from the Mo/C catalysts (17). Furthermore, it was observed that the decline in thiophene HDS activity of the Ni–Mo/C catalysts during a

2-h run time became smaller with increasing Ni/Mo ratios, resembling the situation for the Ni/C catalysts. These activity characteristics are not in favor of explanation (i).

With regard to the second possibility it should be noted that the Ni sulfide particles in Ni/C are inhomogeneously distributed and that the high Ni concentration in the outer part of the support particles may have led to larger Ni sulfide particles and thus to a lower specific surface area and a lower thiophene HDS activity. A similar inhomogeneous distribution has also been reported for Co/C (17) and Fe/C (22) catalysts. The maldistribution resulted from an electrostatic repulsion between the partly protonated carbon surface, due to the slightly acidic nature of the Co and Fe nitrate solutions, and the positively charged Co and Fe ions. The weak adherence of the Co and Fe ions to the support leads to a transport of these species from the inner pores toward the outer pores of the support grains during the drying procedure. This will be most pronounced for an impregnation solution with a low viscosity, at low metal salt concentrations (22–24). The same mechanism should be valid for the Ni/C catalysts. We checked this on a Ni/C catalyst prepared by impregnation of the carbon carrier with $Ni(NH_3)_6^{2+}$ in an ammoniacal solution. The Ni-to-C XPS intensity ratio of this catalyst in the oxidic state (see Fig. 4) was indeed considerably closer to the intensity ratio predicted for monolayer dispersion than that of the Ni/C catalysts prepared with Ni nitrate solutions, implying a more homogeneous dispersion. The Ni-to-C XPS intensity ratios decreased drastically upon sulfidation (see Fig. 4), a phenomenon that was also observed for Co/C catalysts and that was explained as resulting from sintering during sulfidation (17). This sintering behavior reflects the rather weak interaction of the carbon surface with the deposited metal particles (17, 22, 28). The observation that the Ni-to-C intensity ratios of the sulfided Ni/C catalysts remain nearly constant from 0.6 wt% Ni up to approximately 6 wt% Ni can

be explained by assuming that XPS can only detect the outer shell of the catalyst grains and that this shell already contains the maximum amount of Ni at a loading of 0.6 wt% Ni. Additional amounts of Ni will be deposited in the inner parts of the support grains and will, consequently, not alter the Ni-to-C XPS intensity ratio. Thus especially at low loadings the Ni sulfide particles will be highly inhomogeneously distributed.

Since the data points at low Ni contents are crucial in accurately determining the slope at 0 wt% Ni, and since the Ni is least homogeneously distributed at low loadings, the calculated specific Ni activity might indeed be too low. Three observations, however, do not support this explanation. First, the thiophene HDS activity of a more homogeneously dispersed Ni/C catalyst (prepared by impregnation of $Ni(NH_3)_6^{2+}$ in an ammoniacal solution) is exactly equal to that to be expected for a conventially prepared Ni/C catalyst (cf. Fig. 1), indicating that an inhomogeneous dispersion is not necessarily unfavorable for the thiophene HDS activity. Second, graphite-supported Ni sulfide catalysts, which consist essentially of homogeneously dispersed sulfide particles, were found to have nearly identical specific HDS activities per mol Ni as the activated carbon-supported Ni catalysts. Third, the Co/C catalysts are also inhomogeneously dispersed (17). It thus looks as if the inhomogeneous distribution of the Ni sulfide particles in the Ni/C catalysts does not harm the specific Ni activity. A question that remains, however, is whether the percentage of exposed Ni atoms in the Ni/C catalyst extrapolated to 0% Ni loading is the same as in the Ni–Mo/C catalyst. There is little doubt that at low Ni loading all Ni atoms in the Ni–Mo/C catalyst are in the Ni–Mo–S state and fully dispersed on the MoS_2 surface (14, 15). However, whether the Ni sulfide particles in the Ni/C catalyst are small enough for all Ni atoms to be exposed seems doubtful.

Since it is not possible to measure particle sizes with XPS when the particles are inhomogeneously distributed, we tried to determine the size of the Ni_3S_2-like particles by oxygen chemisorption measurements. However, as can be seen from Figs. 1 and 2, the DOC values and the HDS rate constants did not follow the same trend. Whereas the DOC values increased linearly with Ni loading, albeit that they only became measurable above a loading of 0.6 wt% Ni, the rate constants leveled off at higher Ni loadings. The dissimilar behavior of DOC and k values indicates that the DOC values cannot be used to determine the dispersion of the Ni sulfide particles. Probably corrosive chemisorption has taken place, so that not only the outermost Ni atoms, but also subsurface Ni atoms consume oxygen. Even the slope of 0.37 oxygen atoms per Ni atom of the DOC curve suggests that a reaction of the whole Ni_3S_2 particle has taken place, e.g., $Ni_3S_2 + \frac{1}{2}O_2 \rightarrow 2NiS + NiO$. This slope is similar to the one found by Bachelier et al. in their DOC measurements on sulfided Ni/Al_2O_3 and Ni–Mo/Al_2O_3 catalysts (11). The Ni–Mo/C catalysts did not show a correlation between O_2 chemisorption and HDS activity either. Their DOC values increased continuously with Ni contents (Fig. 2), while the HDS rate constants went through a maximum (Fig. 1). We conclude that oxygen chemisorption cannot be used for the quantitative measurement of the active surface area of sulfided Mo and Ni–Mo catalysts, which is in agreement with previous conclusions reached by Zmierczak et al. for sulfided Co–Mo/Al_2O_3 catalysts (29).

The third possible explanation for the difference in the specific activities per Ni atom for the Ni/C and Ni–Mo/C catalysts is that the local structure of the Ni atoms in Ni/C is different from that in Ni–Mo/C and that therefore the Ni sulfide in a Ni/C catalyst is not a good model for the Ni–Mo–S structure in a Ni–Mo/C catalyst. The XPS results (S/Ni stoichiometries and Ni $2p_{3/2}$ binding energies) and the chemical sulfur analyses show that the Ni phase in the sulfided Ni/C catalysts has all the appearances of a Ni_3S_2 phase. This is consistent with the fact that Ni_3S_2 is the most stable compound under

HDS reaction conditions and in the presence of an inert support like carbon (30), and with the EXAFS observations of Louwers and Prins (15), which showed that sulfided Ni supported on LONZA HSAG 300 carbon had the same Ni–S and Ni–Ni distances as Ni_3S_2. In pure Ni_3S_2 every Ni atom is tetrahedrally surrounded by 4 S atoms at 2.24 Å. The Ni EXAFS on Ni–Mo–S/C and Ni–Mo–S/Al_2O_3 catalysts (14, 15) demonstrated that in the Ni–Mo–S structure the Ni atom is surrounded by 5 S atoms at 2.22 Å and about 1 to 2 Mo atoms at 2.84 Å. These observations were explained by a square pyramidal Ni coordination at the edges of the MoS_2 crystallites. It thus seems as if the local structure of the Ni atoms in Ni/C is indeed different from that in the Ni–Mo–S structure and that Ni/C catalysts are therefore not the appropriate model compounds. It should be noted, however, that although the Ni/C catalysts contain Ni_3S_2-like particles, the Ni atoms at the surface of these particles do not need to have a tetrahedral sulfur coordination and may have a square pyramidal coordination. Unfortunately, questions like this will probably stay unanswered for some time to come.

The inadequacy of Ni/C as model compound for Ni–Mo/C catalysts raises the question of whether sulfided Co/C can still be seen as a good model compound for Co–Mo/C catalysts, as suggested by the good agreement between the specific catalytic activities of Co/C and Co–Mo/C catalysts (17). EXAFS investigations (13) have shown that Co/C catalysts contain Co_9S_8-like particles and in pure Co_9S_8 eight-ninths of the Co atoms are tetrahedrally surrounded by S atoms at 2.20 Å and one-ninth of the Co atoms is octahedrally surrounded by S at 2.36 Å. The Co atoms in the Co–Mo–S structure are, like the Ni atoms in the Ni–Mo–S structure, surrounded by 5 S atoms at 2.22 Å and by 2 Mo atoms at 2.80 Å (13). Therefore, if the surface atoms of the Co_9S_8-like structure in Co/C catalysts have a similar local structure as the respective bulk Co atoms, that is tetrahedral or octahedral, then the local structure of the surface Co atoms in Co/C is different from that in the Co–Mo–S structure and Co/C catalysts are actually not suitable as model compounds.

On the other hand, sulfided Co/C and Co–Mo/C catalysts were shown to have similar Mössbauer spectra (18, 19), indicating that their Co atoms were in similar environments. The Mössbauer experiments also showed that the Co/C spectrum was dependent on the pretreatment in 10% H_2S in H_2 and that after sulfiding for 1 h at 300°C the spectrum had partly changed to that of Co_9S_8. It might well be that on a carbon support under mild pretreatment conditions first γ-CoS is formed, which is a metastable cobalt sulfide phase with the millerite structure, in which every metal atom has a square pyramidal fivefold sulfur coordination (31). Under more drastic conditions this γ-CoS then transforms into Co_9S_8. This would explain the Mössbauer results (18, 19), as well as the EXAFS results (13). After 1 h sulfiding at 400°C part of the cobalt was in the Co_9S_8 form and part in the form with a Mössbauer spectrum like that of Co–Mo–S (18, 19). It might therefore well be that (part of) the surface Co atoms still have a square pyramidal structure and that therefore the Co/C and Co–Mo/C catalysts have about the same specific catalytic activity (17).

While the question of the local structure of the surface Co atoms in sulfided Co/C catalysts has not yet been fully answered, it can be studied and is studied by several techniques. The situation for Ni/C catalysts is less favorable and therefore the question as to whether the Ni atoms in sulfided Ni–Mo/C catalysts are the actual active sites, cannot presently be answered.

CONCLUSIONS

Detailed information on the structure of the nickel sulfide phase in carbon-supported Ni and Ni–Mo sulfide catalysts has been obtained by using XPS, dynamic oxygen chemisorption, and chemical sulfur analysis techniques. It is found that the Ni sulfide phase in sulfided Ni/C catalysts consists of Ni_3S_2-like particles that are highly inhomo-

geneously dispersed over the carbon carrier surface, especially at low Ni contents. However, it is concluded that an inhomogeneous distribution is not necessarily unfavorable for thiophene HDS activity. The Ni/C and Ni–Mo/C catalysts showed at low Ni loadings a similar linear relationship of activity versus loading as the DOC values, but at high loadings the activity-loading curves had a convex curvature. The DOC values of both series of catalysts can be well explained by full oxidation of the Ni atoms.

The specific thiophene HDS activity of optimally dispersed Ni in sulfided Ni/C catalysts was much smaller than that of Ni in promoted Ni–Mo/C catalysts. Thus, in contrast to cobalt, it seems as if the increased activity of Ni–Mo/C compared to Ni/C cannot be ascribed to the Ni atoms only. On the other hand, since the local structure, and hence the HDS activity, of the Ni atoms is different in the Ni/C catalysts from that in the Ni–Mo/C catalysts, the question as to whether the Ni atoms in the sulfided Ni–Mo/C catalysts are the actual active sites cannot be answered unambiguously.

REFERENCES

1. Prins, R., de Beer, V. H. J., and Somorjai, G. A., *Catal. Rev. Sci. Eng.* **31**, 1 (1989).
2. Candia, R., Clausen, B. S., and Topsøe, H., *J. Catal.* **77**, 564 (1982).
3. Wivel, C., Candia, R., Clausen, B. S., Mørup, S., and Topsøe, H., *J. Catal.* **68**, 453 (1981).
4. Topsøe, H., Clausen, B. S., Burriesci, N., Candia, R., and Mørup, S., *in* "Preparation of Catalysts II" (B. Delmon, P. Grange, P. Jacobs, and G. Poncelet, Eds.), p. 479. Elsevier, Amsterdam, 1979.
5. Topsøe, H., Clausen, B. S., Candia, R., Wivel, C., and Mørup, S., *Bull. Soc. Chim. Belg.* **90**, 1189 (1981).
6. Topsøe, H., Candia, R., Topsøe, N.-Y., and Clausen, B. S., *Bull. Soc. Chim. Belg.* **93**, 783 (1984).
7. Clausen, B. S., Mørup, S., Topsøe, H., and Candia, R., *J. Phys. Colloq.* **37**, C6-249 (1976).
8. Mørup, S., Clausen, B. S., and Topsøe, H., *J. Phys. Colloq.* **40**, C2-88 (1979).
9. Topsøe, N.-Y., Topsøe, H., Sørensen, O., Clausen, B. S., and Candia, R., *Bull. Soc. Chim. Belg.* **93**, 727 (1984).
10. Topsøe, N.-Y., and Topsøe, H., *J. Catal.* **84**, 386 (1983).
11. Bachelier, J., Duchet, J. C., and Cornet, D., *J. Catal.* **87**, 283 (1984).
12. Bachelier, J., Tilliette, M. J., Duchet, J. C., and Cornet, D., *J. Catal.* **87**, 292 (1984).
13. Bouwens, S. M. A. M., van Veen, J. A. R., Koningsberger, D. C., de Beer, V. H. J., and Prins, R., *J. Phys. Chem.* **96**, 123 (1991).
14. Bouwens, S. M. A. M., Koningsberger, D. C., de Beer, V. H. J., Louwers, S. P. A., and Prins, R., *Catal. Lett.* **5**, 273 (1990).
15. Louwers, S. P. A., and Prins, R., *J. Catal.*, in press.
16. Duchet, J. C., van Oers, E. M., de Beer, V. H. J., and Prins, R., *J. Catal.* **80**, 386 (1983).
17. Vissers, J. P. R., de Beer, V. H. J., and Prins, R., *J. Chem. Soc. Faraday Trans. 1* **83**, 2145 (1987).
18. van der Kraan, A. M., Crajé, M. W. J., Gerkema, E., Ramselaar, W. L. T. M., and de Beer, V. H. J., *Appl. Catal.* **39**, L7 (1988).
19. van der Kraan, A. M., Crajé, M. W. J., Gerkema, E., Ramselaar, W. L. T. M., and de Beer, V. H. J., *Hyperfine Int.* **46**, 567 (1989).
20. Bachelier, J., Duchet, J. C., and Cornet, D., *J. Phys. Chem.* **84**, 1925 (1980).
21. Wagner, C. D., Riggs, W. M., Davis, L. E., Moulder, J. F., and Muilenberg, G. E., "Handbook of X-ray Photoelectron Spectroscopy." Perkin–Elmer Corp., 1979.
22. Groot, C. K., van der Kraan, A. M., de Beer, V. H. J., and Prins, R., *Bull. Soc. Chim. Belg.* **93**, 707 (1984).
23. Ramselaar, W. L. T. M., Nussbaum, R. H., and van der Kraan, A. M., in press.
24. Ramselaar, W. L. T. M., Hadders, R. H., Gerkema, E., de Beer, V. H. J., van Oers, E. M., and van der Kraan, A. M., *Appl. Catal.* **51**, 263 (1989).
25. Ng, K. T., and Hercules, D. M., *J. Phys. Chem.* **80**, 2094 (1976).
26. Broutin, P., Ehrhardt, J. J., Pentenero, A., and Gras, J. M., *J. Microsc. Spectrosc. Electron.* **9**, 57 (1984).
27. Kuipers, H. P. C. E., *Solid State Ionics* **16**, 15 (1985).
28. Vissers, J. P. R., Scheffer, B., de Beer, V. H. J., Moulijn, J. A., and Prins, R., *J. Catal.* **105**, 277 (1987).
29. Zmierczak, W., Muralidhar, G., and Massoth, F. E., *J. Catal.* **77**, 432 (1982).
30. Burch, R., and Collins, A., *J. Catal.* **97**, 385 (1986).
31. Baroni, A., *Atti X Congr. Int. Chim.* **2**, 586 (1938).